Title:

Swimming angle and target strength of larval Japanese anchovy (*Engraulis japonicus*)

Running Title: Swimming angle and target strength of larval Japanese anchovy

Authors and their Affiliations: Yusuke Ito, Hiroki Yasuma, Reiji Masuda, Kenji Minami, Ryuichi Matsukura, Saho Morioka, Kazushi Miyashita

Y. Ito

Laboratory of Marine Ecosystem Change Analysis, Graduate School of Environmental Science, Hokkaido University, 3-1-1 Minato-cho, Hakodate 041-8611, JAPAN

Tel: 81-138-40-8817

Fax: 81-138-40-8856

e-mail: i-you@ees.hokudai.ac.jp

H. Yasuma, K. Miyashita

Laboratory of Marine Ecosystem Change Analysis, Field Science Center for Northern Biosphere, Hokkaido University, 3-1-1 Minato-cho, Hakodate, Hokkaido 041-8611, JAPAN

R. Masuda, K. Minami

Fisheries Research Station Kyoto University, Nagahama, Maizuru, Kyoto

625-0086, JAPAN

R. Matsukura

National Research Institute of Fisheries Engineering, FRA, 7620-7 Hasak, Kamisu, Ibaraki 314-0408, JAPAN

S. Morioka

Fisheries Research Institute, Tokushima Agriculture, Forestry and Fisheries Technology Support Center, 1-3, Hiwasa, Minami, Kaifu, Tokushima, 779-2304, JAPAN

Abstract

The swimming angle of larval Japanese anchovy (*Engraulis japonicus*) was measured in a tank, and target strength (TS) was calculated using a theoretical scattering model. The mean swimming angle was 12.8° (s.d. = ±22.1). Increased speeds of flow led to increased mean swimming angles. The mean swimming angle at flow of 5 cm s^{-1} was higher than those at other speeds. TS values were estimated using a distorted-wave Born approximation model for two cases. Average values were 1–3 cm s^{-1} (Case 1: 11.5° ±22.1) and 5 cm s^{-1} (Case 2: 16.6° ±21.7) for cases 1 and 2, respectively. For case 1, TS ranged from -92.0 to -74.7 dB with a mean of -79.4 dB at 120 kHz. For case 2, TS ranged from -92.2 to -75.2 dB with a mean of -79.9 dB. The mean TS in case 2 was lower than that in case 1, with the maximum difference being 1.0 dB at 120 kHz [standard length: 22.0 mm]. However, there were no significant differences between the regression lines of cases 1 and 2. Thus, changes in flow speed altered the swimming angle of larval Japanese anchovy, but had little influence on TS.

Key words: larval Japanese anchovy, swimming angle, target strength

Title:

カタクチイワシ(*Engraulis Japonicus*)シラスの遊泳姿勢とターゲットストレングス

Authors and Affiliations:

伊藤祐介 (北大院環)

安間洋樹 (北大フィールド科セ)

益田玲爾 (京大フィールド研セ)

南憲吏 (京大フィールド研セ)

松倉隆一 (水研セ水工研)

守岡佐保 (徳島農水総技セ)

宮下和士 (北大フィールド研セ)

Abstract:

カタクチイワシシラスのような無鰾魚を対象に音響計測を実施する場合,わずかな姿勢角変化がターゲットストレングスに大きく影響する.本研究では,頭部を上向きにした状態で遊泳する傾向が強いこと(平均12.8°,標準偏差±22.1),流速が上昇するとこの傾向が強くなることを明らかにした.また,分散分析により姿勢角結果を 2 ケースに分け TS を平均化したが,両者にほとんど差はみられなかった. したがって,物理環境により遊泳姿勢にわずかな違いが生じても,標準偏差が高い場合は平均化 TS への影響は小さいと考えられた.

Introduction

The Japanese anchovy (*Engraulis japonicus*) is one of the most important coastal fisheries species in Japan. The larvae are an especially important resource in near-shore fisheries. According to annual fishery statistics, commercial tow-net harvests were valued at 30 billion yen in 2007 [1]. Therefore, data on the distribution and abundance of larvae are important for near-shore fisheries. Accurate quantitative data on larvae are particularly important, not only for appropriately managing larvae fisheries but also for predicting the recruitment and management of adults.

Various studies have used commercial catch data to estimate the abundance and distribution of larval anchovy, often as linked to environmental parameters such as current, salinity, and precipitation [2, 3, 4]. However, such analyses must use data collected over a long period (months or years), and it is thus difficult to obtain quantitative estimates within a single fishery season. Conversely, acoustic observations using quantitative echo-sounders can provide quantitative data in a short term and have been used for stock assessments of many species [5, 6].

In acoustic surveys, a quantitative echo sounder provides reflections from a fish school at various echo intensities. This acoustic reflection is converted to quantitative data (e.g., number of individuals, biomass) using the target strength (TS). Recently, the TSs of various species has been reported for use in estimating abundance in the field [7, 8]. A split-beam echo sounder can be used to measure TS, if a target is not too small in comparison with wave length. In larval anchovy, however, field

measurement of TS is difficult. Acoustic reflections from larval anchovy are weak because of the small size of the fish and they form school during the day influence the way the target detects them. Therefore, the TS of larval Japanese anchovy should be estimated using a theoretical sound-scattering model.

Many theoretical models have been developed for calculating the TS of fish [9]. Most of these models use an approximate geometric configuration to represent the swim-bladder (in swim-bladdered fish) or body (in swim-bladderless fish) of the target species, which can be obtained from the relationship between TS and swimming angle (pitch or yaw). The Japanese anchovy is a physostomous fish. The swim-bladders of their larvae are filled with gas during the night, which helps to reduce energy consumption. However, during the day, they discharge gas from their swim-bladders and form schools [10]. Miyashita [11] reported that acoustic surveys of larval anchovy should be conducted on high-density schools during the day. Moreover, larval anchovy TSs of 50 and 200 kHz were estimated using the DWBA-based deformed cylinder model (DWBA model) [12, 13] that was developed for swim-bladderless species. This study suggested that the dorsal average TS is very sensitive to changes in tilt angle. Therefore, the TS should be determined using the tilt angle distribution after observation of swimming behavior.

In this study, we observed the swimming angles of larval Japanese anchovy using a video camera and estimated the TS as a function of tilt angle (TS_{avg}) for use in acoustic surveys. We used the swimming angle observation results to calculate the TS_{avg} at 38 and 120 kHz (which are the

main frequencies used by coastal research vessels in Japan) using the DWBA model. We also considered the availability of TS_{avg} as a scale factor in acoustic surveys, using the relationship between TS_{avg} and the body lengths of larval anchovies.

Materials and Methods

Observation of swimming behavior

In January and December 2008, live larval anchovy were provided from fixed shore nets in Wakasa Bay. During both experimental periods, the larvae were transferred as soon as possible to a black fiberglass cylindrical tank (500 L, 116 cm diameter, 77 cm deep) at the Fisheries Research Station of Kyoto University. One day later, we chose live larval anchovy and transported them to an experimental tank which was maintained at ambient temperature (10℃) in an environment that blocked natural light. A 12-h photoperiod was maintained without a dawn or dusk transition in light intensity. During the day, incident light at the surface measured approximately 350 lx; no light was provided during the night.

We conducted the swimming experiment during the day; to simulate the environmental conditions in the bay, and to adjust the flow in the experimental tank seawater was added as needed. The speed of flow was measured before and after video recoding using the Electromagnetic flow velocity (AEM1-D; ALEC Electronics Corp., Tokyo) within the camera field angle. Video recording began 10 minutes after the speed of flow was

stable and lasted for 1 hour at each speed.

Video recordings of the swimming behavior of 40 individuals were collected using two underwater cameras (T-WATER-2200c; HERO, Tokyo) (TL: 39.0±3.4 mm) in January. In December, two Digital HD video camera recorders (HDR-SR12; SONY Corp., Tokyo) were used to give high quality image results for 12 individuals (total length: 39.2±1.8 mm). Recording systems were placed at a depth of 45 cm (Fig. 1), and two additional underwater cameras were used to check the relationships between individuals and the camera lenses. In this environment, we observed the swimming behavior of larval anchovies. The obtained video recordings were converted to photographs at 1-minute intervals for each experimental period. Swimming angles were calculated from these photographs using image editing software (SCM Measure; Moritex Corp., Tokyo) (Fig. 2). There were two requirements for measurements: the centerline of the individual being measured could not be bending, and the individual had to be horizontal from the point of view of the camera lens. The second parameter was confirmed using the dorsal camera. The swimming angle was computed according to the above parameters. The angle was that between the centerline of the fish, an imaginary line running from the root of the tail to the tip, and the true horizontal. We defined positive angles as those for which the fish was head-up and negative angles as those for which the fish was head-down.

Theoretical model

A total of 200 larval anchovy ranging from 18.0 to 35.7 mm SL (SL =

1.22*TL-2.41, R^2=0.99) were used for the TS calculation. The sound scattering from specimens was estimated using the DWBA model. A modification of the Matlab codes described in McGehee et al. [14] ver. 6.1 (MathWorks, Natick, MA) was used to estimate the TS of the deformed cylinder, given as

$$f_{bs} = \int_{\vec{r}_{pos}} \frac{k_{SW}^2 a_c}{4k_{animal}} \left(\frac{1+h^2}{gh^2} - 2 \right) \times e^{2ik_{animal} \cdot \vec{r}_{pos}} \frac{J_l\left(2k_{animal} a_c \cos\beta_{tilt}\right)}{\cos\beta_{tilt}} \left| d\ \vec{r}_{pos} \right| \quad (1)$$

where $f_{(bs)}$ is the complex backscattering amplitude, the relation to backscattering cross-section σ_{bs} is given by $\sigma_{bs} = |f_{bs}|^2$, r_{pos} is the position along the axis of the deformed cylinder, and k is the acoustic wave number given by $k = 2\pi/\lambda$, where λ is the acoustic wavelength. The subscript *sw* refers to the surrounding seawater, the subscript animal refers to larval anchovy, J_l is a Bessel function of the first kind of order l, and a_c is the cross-section radius of the cylinder and incident wave. We digitized and obtained 200 sets of r_{pos} and a_c from the dorsal images of specimens. We tried to measure the density contrast (g) and sound-speed contrast (h) of the larval anchovy using the density-bottle [16] and time-of-flight [17] methods. These values were applied to the DWBA model as parameters (g= 1.068, h= 1.037) [Ito *et al.*, unpublished]. TS (dB) is defined as $TS = 10\log_{10}(\sigma_{bs})$, and the average TS was defined as the mean TS, ranging from -90° to 90° at 1° steps (tilt angle: head-down, head-up position).

The tilt-averaged TS (TS_{avg}) was calculated using the probability density

function (PDF) of fish tilt angle $f_{(bs)}$ in Equations (2) and (3) [15]:

$$\sigma_{Avg} = \int_{-\pi/2}^{\pi/2} \sigma(\theta) f(\theta) d\theta \quad (2$$

$$TS_{Avg} = 10log \ \sigma_{Avg} \quad (3$$

where θ represents swimming angle; $f(\theta)$ was assumed to be a truncated normal distribution function. The truncations were made at $\bar{\theta} - 3S_\theta$ and $\bar{\theta} + 3S_\theta$, where $\bar{\theta}$ and S_θ denote the mean and standard deviation of the tilt angle, respectively. Since the number of samples was different in each photograph. Strictly, we should extract the same number of samples from each photograph. However, we were not able to extract it because the experiment was limited. Therefore, mean swimming angle and standard deviation were calculated using those limited samples in this study.

Results

Theoretical TS

Typical examples of the relationship between variations in TS and body tilt angle at 38 and 120 kHz obtained by the DWBA model are shown in Fig. 3. The variation in TS versus tilt angle showed peaks at about 0° (dorsal) at both frequencies, and the maximum TS at 120 kHz was higher than those at 38 kHz in all specimens. Moreover, these peaks were relatively sharp, especially for the higher frequency, suggesting that slight changes in fish tilt angles have a major effect on TS. The maximum TSs at the 120 kHz were -85.6 dB and -68.1 dB in the smallest and the largest individuals,

respectively. In individuals with larger standard length, the tilt angle had a considerable impact on TS.

Relationship between swimming angle and flow speed

The flow speeds in an experimental tank were 1, 2, 3, 5 cm s^{-1}, respectively. We extracted 2637 angles (January: 2102, December: 535) from photograph. Fig. 4 shows box plots of the swimming angles at each flow speeds. In this study, the mean and standard deviation of the swimming angle of larval anchovy tended to rise as the flow speed increased. However, the standard deviation was not related to the flow speed. Larval anchovy were affected by flow variations ($P < 0.001$, ANOVA), and the mean swimming angle at 5 cm s^{-1} was higher those under the other flow speeds ($P<0.01$, Tukey-Kramer test). Therefore, we separated the calculations of TS into two cases. One case combined the data from flow speeds of 1 to 3 cm s^{-1} (case 1), and other used data from flow speeds of 5 cm s^{-1} (case 2). Fig. 5 shows histograms of the swimming angles in cases 1 and 2. There were no differences in either the ranges of values between cases 1 and 2 or their standard deviations (22.1 and 21.7 respectively). In contrast, the mean swimming angles differed by more than 5° (case 1: 11.5°, case 2: 16.5°).

Tilt-averaged TS

The values of TS were calculated with respect to fish tilt-angle distribution (PDF), which was used for two values (case 1 and case 2) at two

frequencies (38 and 120 kHz). TS values are plotted in Fig. 6as functions of fish SL on a logarithmic scale. Ranges of TS_{avg}, and the equations of the regression lines shown in Fig. 6 (the TS-length equation), are shown in Table 1. In general, the results of TS can be expressed in terms of the body length L using the following equation:

$$TS = m \log_{10} L + b \qquad (4$$

Where m and L are constants for a given species. This equation has been a generally accepted description of the way in which mean TS depends on fish length [18]. The slope m and intercept b can be estimated by linearly regressing the TS on log L. In this study, the regression line was fitted to the estimated data using cases 1 and 2. The results were $TS_{avg} = 60.9 \log_{10} L - 107.4$ (R^2=0.93) for case 1, and $TS_{avg} = 60.1 \log_{10} L - 107.5$ (R^2=0.92) for case 2 at 120 kHz. The mean TS_{avg} was -79.4 for case 1 and -79.9 dB for case 2. The difference in each case was 0.98 dB (SL: 22.0 mm) at the maximum. Analysis of covariance (ANCOVA) was used to test for differences in the regression lines. The slopes and intercepts of the relationships did not differ among cases ($p < 0.05$). TS_{avg} at 38 kHz was weak because L was too small for a wavelength.

Discussion

In this study, we used individuals with total lengths of 28.3 to 45.4 mm for the observation experiment. The swimming angles of these individuals tended to be head-up for each speed of flow. However, the relationship between swimming angle and body length was not clear. We conjecture that

the swimming angle of the larvae differs by body length. Hunter [19] showed that the swimming speed of northern anchovy (*Engraulis mordax*) larvae obviously changed with increases in body length. Additionally, Batty [20] noted that the speed of larval herring increased with length. Thus, the swimming abilities and swimming angles of larvae would also change with increases in body length. In juvenile stage, the swimming angle was almost 0° and there was no influence of flow speed on the mean swimming angle （1–5 cm s^{-1} four steps, one way ANOVA, $P>0.05$） [Ito *et al*., unpublished]. Thus, the differences in swimming angle between larvae and juveniles are likely caused by body growth. Blaxter et al. [21], for example, reported that metamorphosis entails the development of fins, resulting in improved swimming ability. Therefore, as the body grows, the swimming angle will be close to 0°. However, the mean swimming angle of individuals in this study would not be changed by body growth because larval anchovy complete metamorphosis at about 40 mm in length. Individuals measuring 20 mm or less in length may swim at various swimming angles. Therefore, an experiment examining the swimming angles of smaller fish is necessary to improve the precision of the TS. However, our results suggest that the influence of the TS of small individuals is low because the TS of the largest individual was significant compared with that of the smallest individual due to changes in fish tilt angles

We suggest that swimming angle gives larval anchovy the ability to swim against the flow and is determined by body length. In this study, body lengths ranged from 28.3 to 45.4 mm and from 36.4 to 41.3 mm in January and December, respectively. The mean swimming angles were 13.6° and

9.6° for each period (t-test $P < 0.05$). Thus, the swimming angle obviously changed with changes in the range of body lengths. However, with the exception of the data gathered at 5 cm s^{-1}, these values were not significantly different between periods. In individuals with small body lengths, the swimming angle relates to the flow. In this study, the flow at 5 cm s^{-1} affected the mean swimming angle, and the TS_{avg} was calculated using the PDF for two cases (1–3 cm s^{-1}, 5 cm s^{-1}). However, the regression lines of the calculated TS_{avg} for the two cases did not differ significantly (Table 1). The Japanese anchovy is widely distributed in the Northwest Pacific under various environmental conditions, and swimming angles under these conditions have not yet been clarified. Therefore, in the future, swimming behavior must be observed under varying speeds of flow. Additionally, it is necessary to continuous measuring the flow speed during the experiment period.

In this study, the TS of larval anchovy clearly depended on changes in the swimming angle, which was in turn determined by body length. In a previous study, the swimming angle of pelagic fish was fixed at the TS of larvae because the swimming angle of the larvae was not known. As a result, the TS_{avg} will become the factor of the error when the abundance was estimated. Therefore, reliable swimming data must be used to calculate TS_{avg} for use in acoustic surveys. Additionally, this study shows that when the swimming angle has a large standard deviation it has little influence on TS_{avg} (Fig.6).

There are also some additional parameters that affect TS. Mikami *et al.* [22] tried to measure the density (g) and sound-speed contrast (h) of *E.*

pacifica, which has no swim-bladder, and thus no air bubbles in the body, between spring and autumn. Their results showed that the maximum TS values for *E. pacifica*, calculated from a theoretical scattering model, changed by about 5 dB from spring to autumn. Furthermore, Matsukura *et al.* [23] suggested that g and h are affected by seasonal changes in lipid profiles. In this study, the larval anchovy g and h values were fixed at 1.068 and 1.037, respectively. However, these values must be changed under varying conditions (i.e., season, area), and we must further examine such parameters in the future.

As mentioned above, these factors are important when attempting to estimate the target strength (TS) of larval Japanese anchovy. In particular, the influence of swimming angle was high. This is the first paper to provide swimming angle data. The TS_{avg} given in Fig. 6 are recommended for use in acoustic surveys of fishing ground areas. Additionally, schools of the larvae of this species can be distinguished from those of other species using the volume back-scattering strength difference method.

Acknowledgements

We thank the captains and crew of Kanagasaki Maru No. 8 for their cooperation in collecting specimens. We also thank Yukio Ueta, Keisuke Mori Fisheries Research Institute, Tokushima Agriculture and the Forestry and Fisheries Technology Support Center for their support in collecting specimens. This study was supported in part by the Fisheries Agency of Japan under the project “Research and development projects for application

in promoting new policy of Agriculture Forestry and Fisheries.” We thank this institution for their support.

References

1. Annual Statistics on Fishery and Aquaculture Production 2006, Statistics Department, Ministry of Agriculture 2006, Forestry and Fisheries, Tokyo. 2008.
2. Saiura K, Takeda Y (2001) Spring fishing ground formation of anchovy, *Engraulis Japonica* larvae in 1999 and 2000 in the Kii Channel. Fisheries Biology and Oceanography in the Kuroshio 2: 109-118 (in Japanese).
3. Morioka S (2006) Trial of spring shirasu (*Engraulis japonicus* larvae) fishery forecast in Kii Channel by using multiple regression analysis. Fisheries Biology and Oceanography in the Kuroshio 7: 21-27 (in Japanese).
4. Mitani I (1988) The biological studies on the larvae of Japanese anchovy, *Engraulis japonica* HOTTUYN, In Sagami Bay. PhD Thesis. University of Hokkaido, Hokkaido (in Japanese).
5. Honda S (2004) Abundance estimation of the young cohorts of the Japanese Pacific population of walleye pollock (*Theragra chalcogramma*) by acoustic surveys. PhD thesis. University of Hokkaido, Hokkaido (In Japanese)

6. Yasuma H (2004) Studies on the acoustical biomass estimation of myctophid fishes. PhD thesis. University of Tokyo, Tokyo (In Japanese)
7. Zhao X, Wang Y, Dai F (2008) Depth-dependent target strength of anchovy (*Engraulis japonicus*) measured *in situ*. ICES J Mar Sci 65: 882-888.
8. Foote KG, Traynor JJ (1988) Comparison of walleye pollock target-strength estimates determined from *in situ* measurements and calculations based on swimbladder form. J Acoust Soc Am 83(1): 9-17.
9. Simmonds J, MacKennan D (2005) Fisheries Acoustics 2nd edn. Blackwell Publishing, Oxford.
10. Uotani I (1973) Diurnal changes of gas bladder and behavior of postlarval anchovy and other related species. Bull Jap Soc Sci Fish 39: 867-876 (in Japanese with English abstract).
11. Miyashita K (2003). Diurnal changes in the acoustic-frequency characteristics of Japanese anchovy (*Engraulis japonicus*) post-larvae “shirasu” inferred from theoretical scattering models. ICES J Mar Sci 60: 532-537.
12. Stanton TK, Chu D, Wiebe PH (1993) Sound scattering by several zooplankton groups. Ⅱ. Scattering models. J Acoust Soc Am 103:236-253.
13. Chu D, Foote KG, Stanton TK (1993) Further analysis of target strength measurements of Antarctic krill at 38 and 120 kHz: Comparison with deformed cylinder model and inference of orientation. J Acoust Soc Am 93: 2985-2988.
14. McGehee D E, O’Driscoll RL Martin Traykovdky LV (1998) Effects of

orientation on acoustic scattering from Antarctic krill at 120 kHz. Deep-Sea Res 45: 1273-1394.

15. Foote KG (1980a). Averaging of fish target strength functions. J Acoust Soc Am 67(2): 504-515.
16. Foote KG (1990). Speed of sound in *Euphausia superba*. J Acoust Soc Am 87: 1405-1408.
17. Greenlaw CF (1977). Backscattering spectra of preserved zooplankton. J Acoust Soc Am 62: 44-52.
18. Foote KG (1979a). On representing the length dependence of acoustic target strengths of fish. J Fish Res Board Can 36(12): 1490-1496.
19. Hunter J R (1972) Swimming and feeding behavior of larval anchovy, *Engrauis mordax*. Fish Bull 70: 821-838.
20. Batty R S (1984). Development of swimming movements and musculature of larval herring (*Clupea harengus*). J exp Biol 110: 217-229.
21. Blaxter J H S, Staines M E (1971). Food searching potential in marine fish larvae. Fourth European marine biological symposium. Cambridge University Press, Cambridge, England.
22. Mikami H, Mukai T, Iida K (2000). Measurements of density and sound speed contrasts for estimating krill target strength using theoretical scattering models. Nippon Suisan Gakkaishi 66(4) 682-689 (in Japanese with English abstract).
23. Matsukura R, Yasuma H, Murase H, Yonezak S, Funamoto T, Honda S, Miyashita K (2009) Measurement of density contrast and sound-speed contrast for target strength estimation of *Neocalanus* copepods

(*Neocalanus cristatus* and *Neocalanus plumchrus*) in the North Pacific Ocean. Fish Sci 75: 1377-1387.

Table 1 Equations for the linear regression in Fig. 5 and mean target strength at each frequency; y represents TS (dB), and x represents the log of standard length in centimeters.

Fig. 1 Schematic diagram of the experimental tank used for the penned Japanese anchovy larvae.

Fig. 2 Typical example of a photograph obtained from the observation experiment. The upper panel shows a dorsal image and the lower shows a lateral image; θ indicates the swimming angle.

Fig. 3 Typical variations in the target strength (TS) of minimum (a) and maximum larval length (b) as a function of fish pitch angle, estimated by the distorted-wave Born approximation (DWBA) model at 38 (dotted lines) and 120 (bold lines) kHz. Positive angles are head-up and negative angles are head-down.

Fig. 4 Box plots of the swimming angles of larval Japanese anchovy. Middle squares indicate the mean; whiskers show the standard deviation. Numbers in parentheses indicate the maximum and minimum values.

Fig. 5 Frequency distributions of the swimming angles of larval Japanese anchovy under flow rates of 1–3 cm s^{-1} (a) and 5 cm s^{-1} (b).

Fig. 6 Relationship between TS and log of standard length (L in mm) each case. TS is 38 kHz for the upper panel and 120 kHz for the lower panel. The circle and cross indicate calculated TSs for cases 1 and 2, respectively. Equations for the regression lines in each panel are given in Table 1.

Table 1 Equations for the linear regression in Fig. 5 and mean target strength at each frequency; y represents TS (dB), and x represents the log of standard length in centimeters.

	n	Frequency (kHz)	Mean TS_{ave} (dB)	y = p x + q			
				p	q	r^2	S.E.
Case 1 (1-3cm/sec)	1955	38	-94.2	67.3	-125.3	0.93	1.5
		120	-79.4	60.1	-107.4	0.92	1.4
Case 2 (5cm/sec)	682	38	-94.5	66.2	-125.1	0.92	1.5
		120	-79.9	60.1	-107.5	0.92	1.4

Fig.1

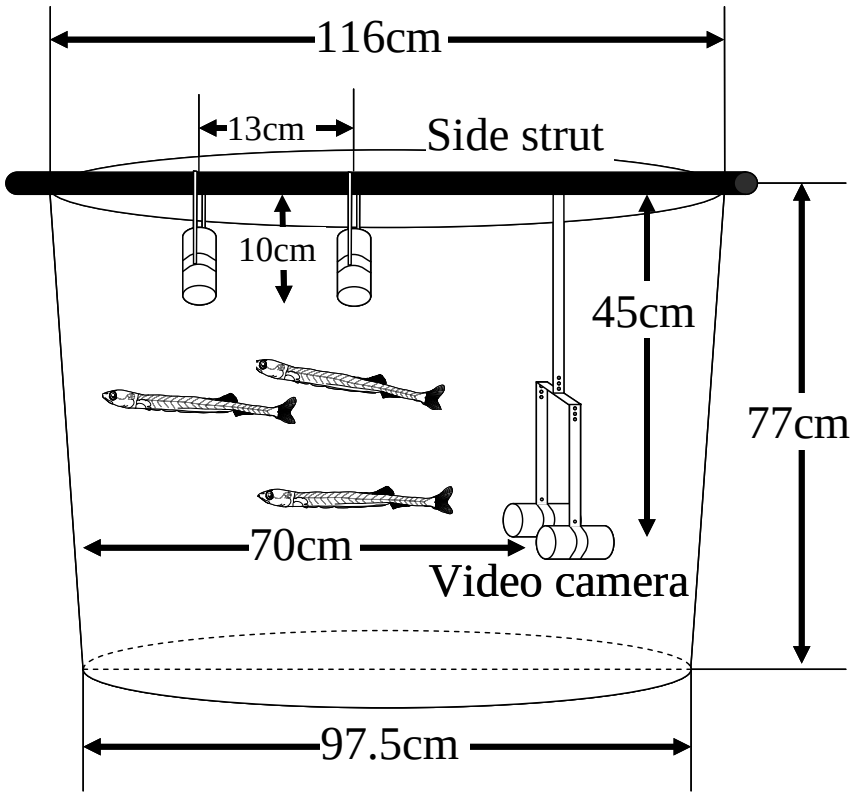
116cm
13cm
Side strut
10cm
45cm
77cm
70cm
Video camera
97.5cm

Fig.2

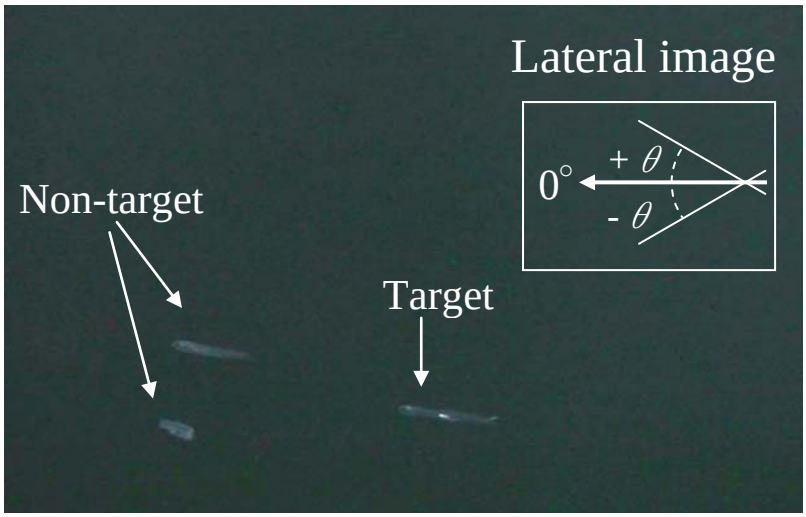

Fig.3

(a)

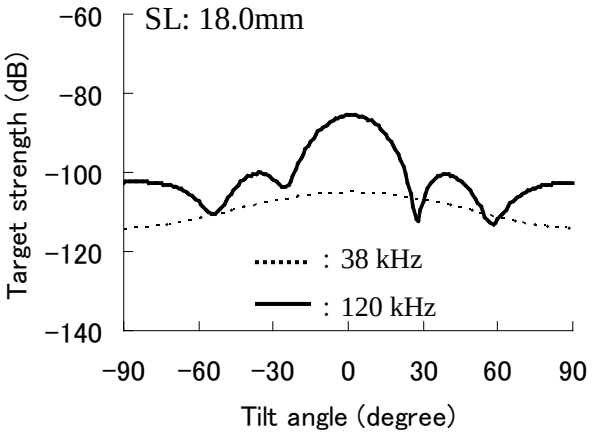
SL: 18.0mm
Target strength (dB)
−60
−80
−100
−120
−140
: 38 kHz
: 120 kHz
−90
−60
−30
0
30
60
90
Tilt angle (degree)

(b)

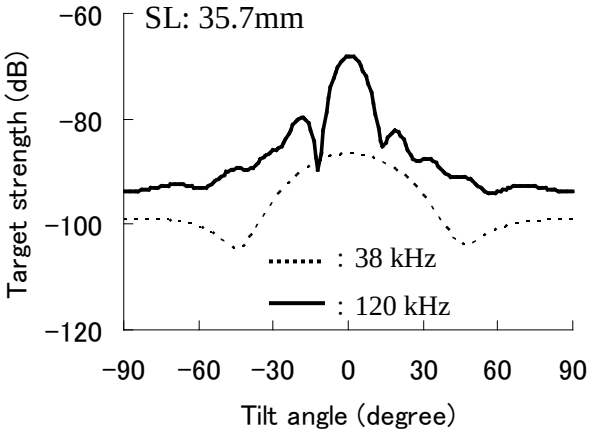
SL: 35.7mm
Target strength (dB)
−60
−80
−100
−120
: 38 kHz
: 120 kHz
−90
−60
−30
0
30
60
90
Tilt angle (degree)

2

Fig.4

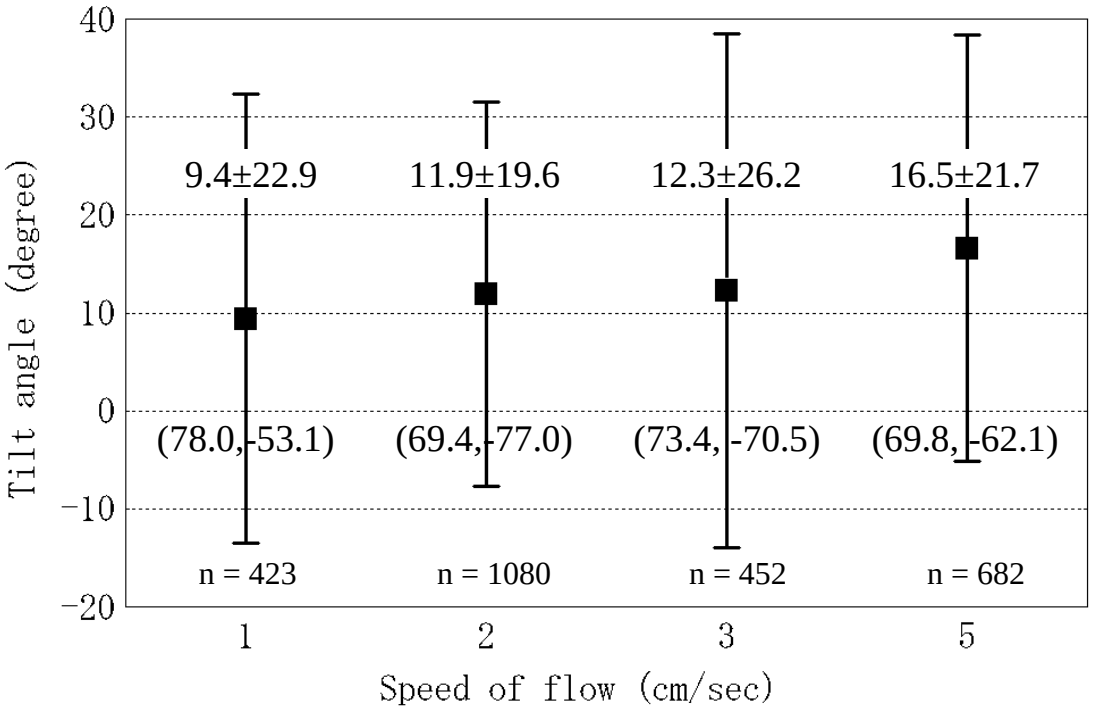
40
30
20
10
0
−10
−20
Tilt angle (degree)
9.4±22.9
11.9±19.6
12.3±26.2
16.5±21.7
(78.0,-53.1)
(69.4,-77.0)
(73.4,-70.5)
(69.8,-62.1)
n = 423
n = 1080
n = 452
n = 682
1
2
3
5
Speed of flow (cm/sec)

Fig.5

(a)

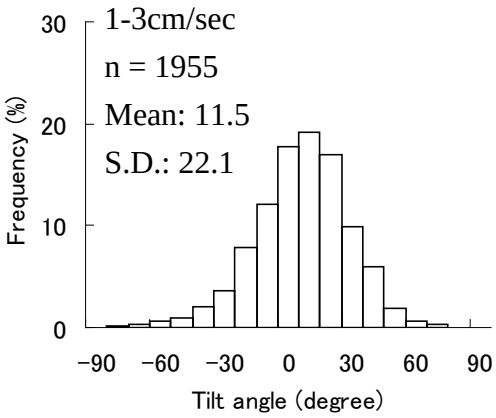
1-3cm/sec
n = 1955
Mean: 11.5
S.D.: 22.1
Frequency (%)
30
20
10
0
−90 −60 −30 0 30 60 90
Tilt angle (degree)

(b)

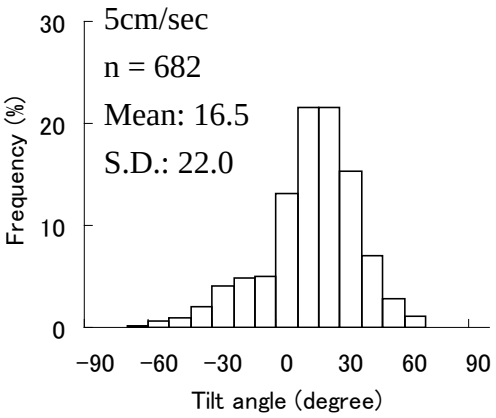
5cm/sec
n = 682
Mean: 16.5
S.D.: 22.0
Frequency (%)
30
20
10
0
−90 −60 −30 0 30 60 90
Tilt angle (degree)

Fig.6

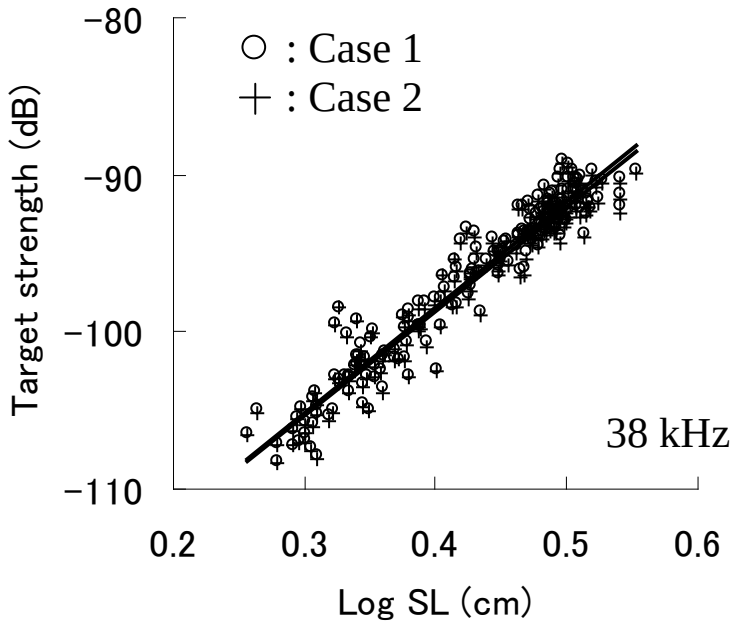
○ : Case 1
＋ : Case 2
38 kHz
Target strength (dB)
−80
−90
−100
−110
0.2
0.3
0.4
0.5
0.6
Log SL (cm)

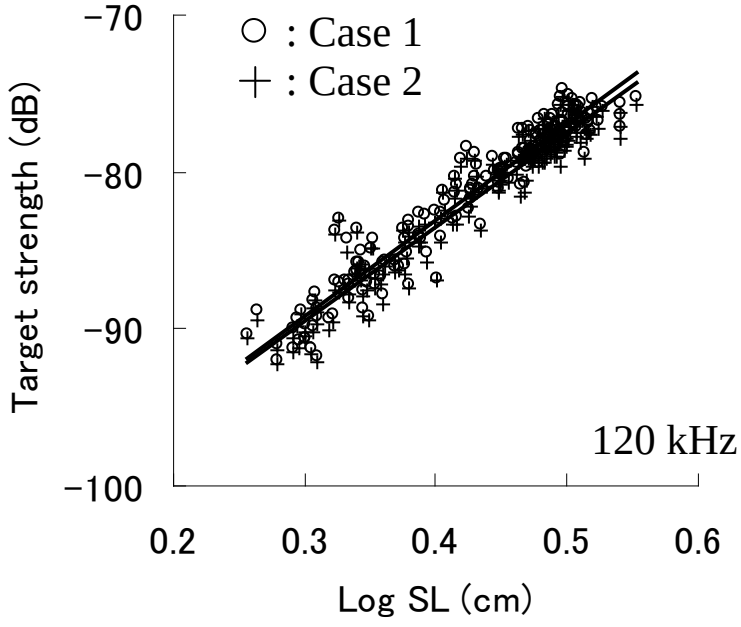
○ : Case 1
＋ : Case 2
120 kHz
Target strength (dB)
−70
−80
−90
−100
0.2
0.3
0.4
0.5
0.6
Log SL (cm)